

RECEIVED

ANL/ET/CP-102227

AUG 04 2000

Fault Current Limiter - Predominantly Resistive Behavior of a BSCCO Shielded-Core Reactor

M. G. Ennis, T. J. Tobin, Y. S. Cha, and J. R. Hull

Abstract—Tests were conducted to determine the electrical and magnetic characteristics of a superconductor shielded core reactor (SSCR). The results show that a closed-core SSCR is predominantly a resistive device and an open-core SSCR is a hybrid resistive/inductive device. The open-core SSCR appears to dissipate less than the closed-core SSCR. However, the impedance of the open-core SSCR is less than that of the closed-core SSCR. Magnetic and thermal diffusion are believed to be the mechanism that facilitates the penetration of the superconductor tube under fault conditions.

Index Terms—fault current limiter, magnetic diffusion, SSCR, transformer model.

INTRODUCTION

In 1974, a consensus of Electric Power Research Institute listed the need for a fault current limiter (FCL) as a top priority research and development (R&D) item [1]. However, almost all the devices considered some two decades ago were either technically or economically unsuccessful. The discovery of high- T_c superconductors more than a decade ago renewed interest in FCLs and there is a worldwide R&D effort aimed at pursuing various concepts of FCLs [2]. A leading candidate of high- T_c FCL is the so-called superconductor shielded core reactor (SSCR). The SSCR is a passive device and consists mainly of a closed iron core inside a superconductor tube and a copper coil wound on the outside of the superconductor tube [3-10]. The SSCR uses the shielding capability of a superconductor tube to keep the inductance low under normal operating conditions. Under fault conditions, the large current in the copper coil exceeds the shielding capability of the superconductor tube and there is a jump in impedance because the iron core is no longer shielded from the coil by the superconductor tube. Originally, it was thought that the SSCR is an inductive device, because the coupling between the superconductor and the primary circuit is magnetic in nature. For some time, however, it has been realized from test results that the SSCR is really a resistive device and the superconductor tube heats up considerably during a fault, and its recovery usually takes much longer than that of an inductive device because heat has to be removed from the superconductor after the fault is cleared. There is still, in general, a lack of understanding of how the superconductor tube behaves both magnetically and

thermally during a fault. In this paper, we report the results of testing a SSCR with both a closed and an open core under symmetric and asymmetric fault conditions. Tests were also conducted to determine the ac steady-state shielding capability of the melt-cast processed BSCCO tube.

TEST SECTION AND SSCR ASSEMBLY

The assembled SSCR is sketched in Fig. 1, illustrating the arrangement of the steel core, the BSCCO tube, the exciting coil and the pickup coil. With the cross-member in place the SSCR is referred to as "closed-core," and with it removed as "open-core." Each core section is about 65 cm^2 , with the two vertical limbs some 25 cm long, having a center-center separation of around 15 cm.

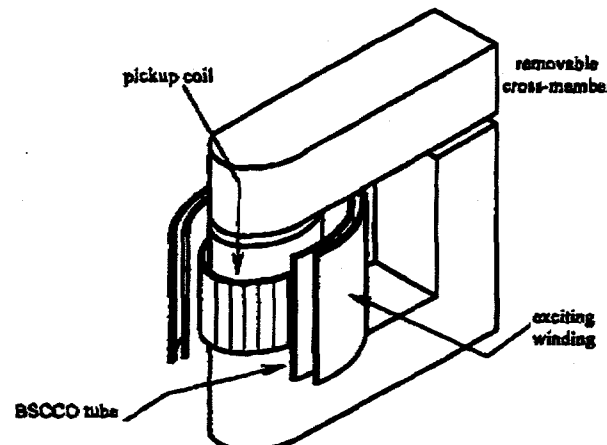


Fig. 1. Two-piece laminated core showing BSCCO tube, exciting and pickup coils and removable cross-member.

The two-piece steel core was made from 0.6-mm-thick laminations of M22 steel, having both coils and the BSCCO tube mounted on one leg of approximately circular cross-section. Each of the two coils comprised 100 turns of magnet wire wound in two layers, the exciting coil (AWG 10) over a profiled fiberglass mandrel, and the pickup coil (AWG 35) directly onto the steel core over a layer of Kapton™ tape. Not shown in the sketch are two bonded-fiber end-rings which act not only to hold the BSCCO tube and exciting coil in place, but also to permit LN_2 to flow into the spaces between the parts. The entire assembly was submerged in LN_2 for the duration of the tests. No special measures were taken to guide the electrical connections out of the cryogenic container, except to prevent excessive mechanical movement during the tests.

The BSCCO tube is supplied by Aventis (formerly Hoechst). The outside diameter of the BSCCO tube is 113 mm and the wall thickness is 6 mm. The axial length of

Manuscript received June 16, 2000. This work was supported in part by the U.S. Department of Energy, Energy Efficiency and Renewable Energy, as part of a program to develop electric power technology, under Contract W-31-109-Eng-38.

M. G. Ennis and T. J. Tobin are with S&C Electric Company, Chicago, IL 60626 (telephone: 773-338-1000, e-mail: mennis@sandc.com).

Y. S. Cha and J. R. Hull are with the Energy Technology Div., Argonne National Laboratory, Argonne, IL 60439 (telephone: 630-232-5899, e-mail: yscha@anl.gov).

DISCLAIMER

This report was prepared as an account of work sponsored by an agency of the United States Government. Neither the United States Government nor any agency thereof, nor any of their employees, make any warranty, express or implied, or assumes any legal liability or responsibility for the accuracy, completeness, or usefulness of any information, apparatus, product, or process disclosed, or represents that its use would not infringe privately owned rights. Reference herein to any specific commercial product, process, or service by trade name, trademark, manufacturer, or otherwise does not necessarily constitute or imply its endorsement, recommendation, or favoring by the United States Government or any agency thereof. The views and opinions of authors expressed herein do not necessarily state or reflect those of the United States Government or any agency thereof.

DISCLAIMER

**Portions of this document may be illegible
in electronic image products. Images are
produced from the best available original
document.**

the tube is 200 mm. To make the tube stronger mechanically, the outside of the tube is coated with a thin layer of fiberglass composite. The manufacturer supplied data indicates that the ac steady-state critical current (maximum shielding capability) of the tube is about 5,000 A.

EXPERIMENTAL RESULTS

The first series of tests were conducted to determine the ac steady-state characteristics of the SSCR and the results are shown in Fig. 2. The vertical coordinate Δt is defined as the time interval from the beginning of the test to the time when current limiting begins. It can be observed that Δt decreases sharply with the system voltage. For system voltage less than 40 V, the superconductor is able to shield the applied magnetic field completely. For very large system voltages (>300 V), field penetration occurs quickly. This observation is consistent with the results reported by Cha and Askew [11], who found that the penetration field depends on the ramp rate of the excitation current. Similar results were also reported recently by Meerovich, et al. [5].

Most of the tests were conducted for a duration of approximately 90 ms (5 cycles at 60 Hz). Typical current and voltage profiles of a 5-cycle test are shown in Fig. 3. For this particular test (closed core), it can be seen that current limitation begins very early (a few milliseconds) in the test. Also shown is the instantaneous power dissipation of the SSCR. The peak power dissipation occurs shortly after significant current limitation and the power dissipation begins to decrease from then on. This is because the induced current in the superconductor tube begins to decrease as the temperature increases. In general, the experimental data show that, after field penetration, the voltage and current are in phase for the closed-core SSCR while the voltage and current are out of phase for the open-core SSCR. The phase angle increases with generator voltage for the open-core tests. This means that the open-core SSCR becomes more inductive as the system voltage increases. From the data on phase angle between V and I and the ratio of $V(\text{peak})/I(\text{peak})$, we can calculate the resistance R and the reactance X_ϕ of the SSCR (assuming sinusoidal wave form). The R and X_ϕ are determined by assuming that these two elements are in parallel.

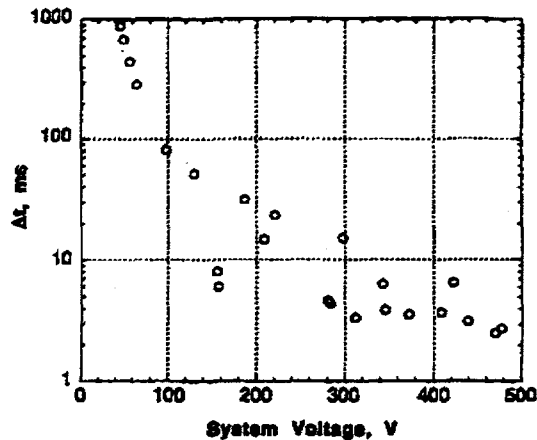


Fig. 2. Variation of Δt (defined as the time interval from the beginning of the test to the time when current limiting occurs) with system voltage.

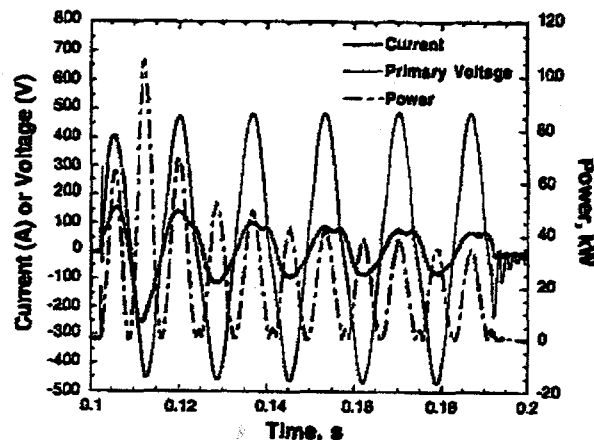


Fig. 3. Typical profiles of current, voltage, and power dissipation of a closed-core SSCR.

CLOSED-CORE TESTS

Figure 4 shows the calculated resistance R of the SSCR as a function of time. The resistance R increases with time and the generator voltage. Figure 5 shows the calculated reactance X_ϕ of the SSCR as a function of time. The reactance increases from a small value at the beginning of the test to very large value (say 100Ω) as time goes on. Initially, both R and X_ϕ are small. As test goes on, both R and X_ϕ increase with time. However, X_ϕ increases much faster than R and soon X_ϕ becomes much larger than R . When this happens, the SSCR becomes a resistive device because all the current is going through R . The abnormal behavior of test 113 in Fig. 5 is probably due to the distortion of wave shape which always occurs at relatively high generator voltage.

OPEN-CORE TESTS

Figures 6 and 7 show the calculated resistance R and reactance X_ϕ , respectively, as a function of time for the open-core tests. The resistance R of the open-core test (Fig. 6) is quite similar to that of the closed-core test (Fig. 4). They both increase with time and are of the same order of magnitude (from one to several Ohms). The reactance X_ϕ of the open-core tests (Fig. 7) showed quite different behavior

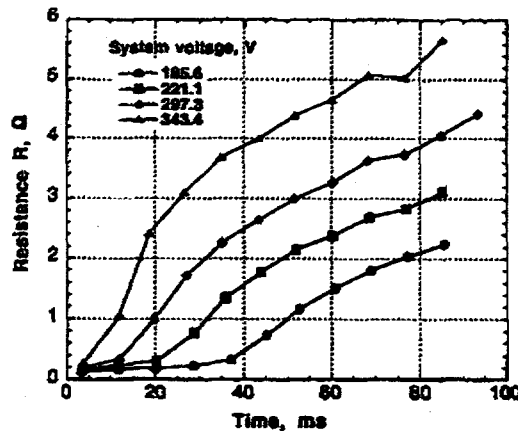


Fig. 4. Calculated resistance R as a function of time for closed-core tests.

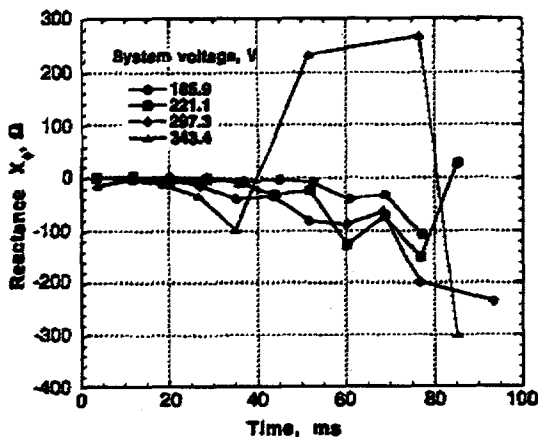


Fig. 5. Calculated reactance as a function of time for closed-core tests.

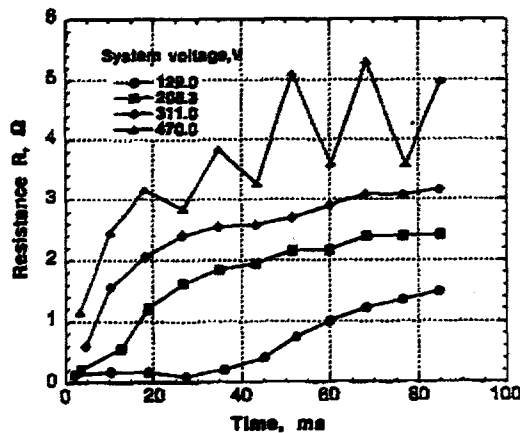


Fig. 6. Calculated resistance R_p as a function of time for the open-core tests.

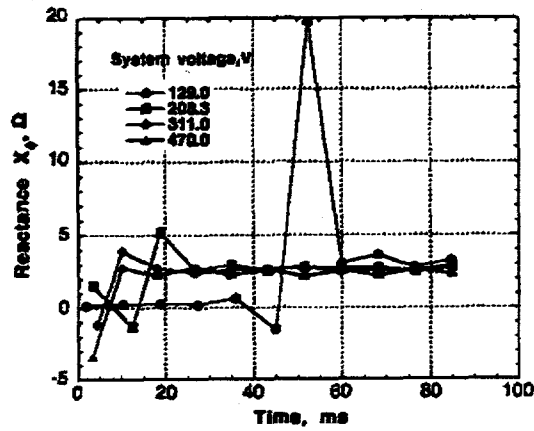


Fig. 7. Calculated reactance as a function of time for the open-core tests.

from that of the closed-core tests (Fig. 5). First, the reactances in the open-core tests are much smaller than those of the closed-core tests. Second, except for the initial period, the reactance in the open-core tests reaches about 3Ω and remains there for the rest of the test, unlike that in the closed-core tests, which continues to increase to very large values (100Ω or higher). Third, the resistance and the reactance are of the same order of magnitude for the open-core tests. Because the open-core SSCR is more inductive, it dissipates

and heats up less than the closed-core SSCR. The disadvantage of the open core is, however, that the inductance is very limited because the effective μ is relatively small compared to that of a closed core. It is not clear why test 129 in Fig. 7 shows the exceptional behavior.

EQUIVALENT CIRCUIT OF THE SSCR

Figure 8 shows the simplified transformer equivalent circuit, where R_p is the core-loss resistance, X_m is the core magnetizing impedance, X_L is the core-leakage reactance, R_2 is the BSCCO tube resistance, R_p is the resistance of the primary winding and X_p its associated reactance.

As can be appreciated from the figure, the SSCR impedance is the total equivalent impedance looking into the terminals of the circuit of Fig. 8. Since in general both R_p and X_p will be both small and constant throughout the operating current range of the SSCR, and the leakage impedance is also small because of the close coupling of the components, then the main influences on the behavior of the device will come from the interaction of the core and BSCCO tube parameters.

Based on core parameters derived from our tests, Fig. 9 shows the variation in the apparent impedance of the SSCR as the tube resistance, R_2 , increases. For very small R_2 , the SSCR impedance is dominated by the leakage impedance of the equivalent transformer. With increasing R_2 , the SSCR quickly becomes resistive, reflecting the changes within the BSCCO tube during the magnetic/thermal diffusion process. Only when R_2 becomes very large does the SSCR again begin to look inductive, reflecting now the magnetizing

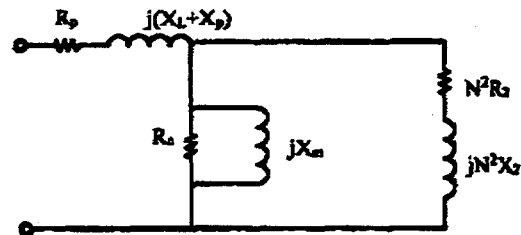


Fig. 8. Equivalent circuit of the SSCR.

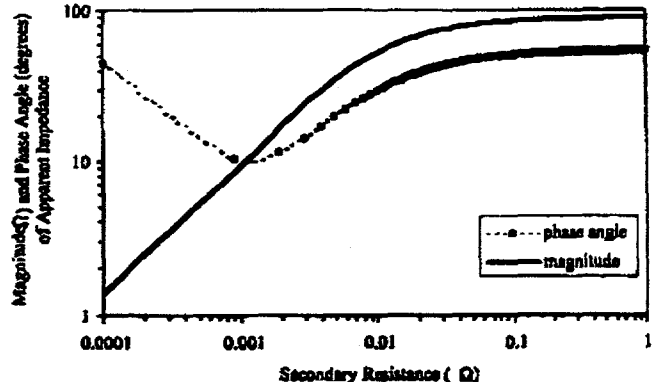


Fig. 9. Variation of the impedance with the resistance of the tube R_2 .

inductance of the laminated steel core. Only when the transition of the BSCCO tube is both fast and very large can the SSCR be tuned in the manner referred to by Paul et al. [12]. Based on the results of our tests, this tunable regime is very difficult to attain, since even in the normal state, the resistance of the BSCCO tube is smaller than the magnetization inductance of the equivalent transformer.

MAGNETIC/THERMAL PENETRATION OF THE SUPERCONDUCTOR TUBE BY THE APPLIED MAGNETIC FIELD

The experimental data clearly demonstrate that the applied field penetrates the superconductor tube because otherwise the transformer model would not have worked so well to explain all the experimental results. We know the results are not entirely due to thermal effects, because the tube is not thermally quenched yet when significant current limiting begins (the total energy dissipated is far below that needed to thermally quench the superconductor tube). We believe that the field penetration is the result of the combined effects of magnetic and thermal diffusion [13]. Magnetic diffusion is enhanced by two factors. First is the current density, which is much larger than the critical current density in a transient experiment. This large induced current will greatly increase the resistivity of the superconductor tube. This will result in increased rate of magnetic diffusion because the diffusion coefficient is linearly proportional to the resistivity. Even without temperature change, magnetic diffusion becomes much faster and the diffusion time becomes comparable to the characteristic time of a 60-cycle system just because the induced current is larger than the critical current during the transient. The second factor that will enhance magnetic diffusion is the temperature rise as a result of dissipation. Temperature increase will also increase the resistivity of the superconductor. This further increases the rate of magnetic diffusion and the superconductor is readily penetrated by the applied field with a characteristic time of a few milliseconds. Thus, the combined effect of increased current density (over the critical current density) and temperature increase due to dissipation facilitated the penetration of the superconductor tube by the applied magnetic field.

SUMMARY AND CONCLUSIONS

The transformer model appears to explain the experimental results quite well both for a closed and an open-core SSCR. The closed-core tests are resistively dominated and the open-core tests are both inductive and resistive. The closed-core SSCR is mostly resistive because the reactance of the primary coil and the unsaturated core is much larger than the reflected resistance of the superconductor tube. The result is that most of the primary current is consumed in the superconductor tube and very little current is needed to magnetize the core. The open-core SSCR is both inductive and resistive simply because the inductance of an open core is much smaller than that of a closed core and primary current is shared between the magnetizing current and the secondary current. The fact that the closed-core SSCR provided a higher impedance than that of an open-core SSCR can be explained by the equivalent circuit shown in Fig 8. The parallel configuration guarantees that the net impedance is smaller than the impedance of either element. Because the inductance of the open-core SSCR remains fairly constant, the net impedance always remains

below that of the closed-core no matter what the reflected resistance is from the secondary circuit. The impedance of the closed-core SSCR, on the other hand, continues to increase with the resistance of the superconductor tube.

Finally, experimental evidence indicates that significant current limiting begins after the applied field has penetrated the superconductor tube. We believe that the field penetration is the result of the combined effect of magnetic and thermal diffusion in the superconductor. Increased current density (over the critical current density) and increased temperature in the superconductor enhance magnetic diffusion. The rate of magnetic diffusion increases with the resistivity of the superconductor. Both the increased current density and the increased temperature will increase the resistivity and facilitate the penetration of the superconductor tube by the applied field.

ACKNOWLEDGMENT

The authors would like to thank R. C Niemann, A. S. Wantrauba of Argonne National Laboratory, and R. P. Mikosz, J. A. Moore, T. Kovanko of S&C Electric, for their assistance in the design, fabrication, and testing of the fault current limiter.

REFERENCES

- [1] M. Rabinowitz, Power Systems of the Future (Part 3), *IEEE Power Engineering Review*, vol. 20, no. 5, May 2000, pp. 21-24.
- [2] R. F. Giese, A worldwide overview of superconductivity development efforts for utility applications, paper presented at the American Power Conference, Chicago, Illinois, April 1996.
- [3] W. Paul, et al., Test of a 1.2 MVA high-T_c superconducting fault current limiter, *Supercond. Sci. Technol.*, vol. 10, 1997, pp. 914-918.
- [4] J. Cave, et al., Development of inductive fault current limiters up to 100 kVA class using bulk HTS materials, *IEEE Trans. Appl. Superconductivity*, vol. 9, no. 2, June 1999, pp. 1335-1338.
- [5] V. Meerovich, et al., Performance of an inductive fault current limiter employing BSCCO superconducting cylinders, *IEEE Trans. Appl. Superconductivity*, vol. 9, no. 4, December 1999, pp. 4666-4676.
- [6] J. Nakatsugawa, et al., Magnetic characteristics of a high-T_c superconducting cylinder for magnetic shielding type superconducting fault current limiter, *IEEE Trans. Appl. Superconductivity*, vol. 9, no. 2, June 1999, pp. 1373-1376.
- [7] Y. S. Cha, et al., Induced current in Bi₂Sr₂CaCu₃O_x superconductor tube, *Applied Superconductivity*, vol. 4, no. 4, 1996, pp. 173-184.
- [8] Y. Bashkirov, et al., Application of superconducting shields in current-limiting and special-purpose transformers, *IEEE Trans. Appl. Superconductivity*, vol. 5, no. 2, June 1995, pp. 1075-1078.
- [9] T. Onishi and A. Nii, Investigation on current limiting performances in magnetic shield type high T_c superconducting fault current limiter, *Cryogenics*, vol. 37, 1997, pp. 181-185.
- [10] M. Joo and T. K. Ko, The analysis of the fault currents according to core saturation and fault angles in an inductive high-T_c superconducting fault current limiter, *IEEE Trans. Appl. Superconductivity*, vol. 6, no. 2, June 1999, pp. 62-67.
- [11] Y. S. Cha and T. R. Askew, Transient response of a high-temperature superconductor tube to pulsed magnetic fields, *Physica C*, 302, 1998, pp. 57-66.
- [12] W. Paul, et al., Tests of a 100 kW high-T_c superconducting fault current limiter, *IEEE Trans. Appl. Superconductivity*, vol. 5, no. 2, 1995, pp. 1059-1062.
- [13] Y. S. Cha, Magnetic diffusion in high-T_c superconductors, *Physica C*, 330, 2000, pp. 1-8.